

1 **Structural integrity monitoring of onshore wind turbine concrete foundations**

2 Magnus Currie^{1*}, Mohamed Saafi^{2*}, Christos Tachtatzis³ and Francis Quail⁴

3 ¹E D P Renewables Ltd, Edinburgh, EH2 2BY, UK

4 ²Department of Engineering, Lancaster University, Lancaster, LA1 4YR, UK

5 ³Department of Electrical and Electronic Engineering, University of Strathclyde, Glasgow, G1 1XW, UK

6 ⁴Aramco Technology Office, Aberdeen, AB32 6FE

7 **Abstract**

8 Signs of damage around the bottom flange of the embedded ring were identified in a large
9 number of existing onshore concrete foundations. As a result, the embedded ring experienced
10 excessive vertical displacement. A wireless structural integrity monitoring (SIM) technique was
11 developed and installed in the field to monitor the stability of these turbines by measuring the
12 displacement patterns and subsequently alerting any significant movements of the embedded
13 ring. This was achieved by using wireless displacement sensors located in the bottom of the
14 turbine. A wind turbine was used as a test bed to evaluate the performance of the SIM system
15 under field operating conditions. The results obtained from the sensors and supervisory control
16 and data acquisition (SCADA) showed that the embedded ring exhibited significant vertical
17 movement especially during periods of turbulent wind speed and during shut down and start up
18 events. The measured displacement was variable around the circumference of the foundation as
19 a result of the wind direction and the rotor uplift forces. The excessive vertical movement was
20 observed in the side where the rotor is rotating upwards. The field test demonstrated that the
21 SIM technique offers great potential for improving the reliability and safety of wind turbine
22 foundations.

23

24 Keywords

25 Onshore wind turbine, Concrete foundations, Forensic investigation, Structural integrity,
26 Monitoring.

27 *Corresponding authors (magnus.currie@gmail.com) and m.saafi@lanacaster.ac.uk

28

29

30 **1. Introduction**

31 Wind is currently considered as one of the most cost-effective large-scale alternative energy
32 sources. In the UK, onshore wind farm developments make up the largest proportion of wind
33 generating capacity, with offshore production beginning to significantly grow. Structural
34 integrity monitoring (SIM) has become an integral part of onshore wind farm asset management
35 programs to ensure safety and reliability. Like any other structure, a wind turbine is prone to
36 damage from fatigue, environmental exposures and construction defects. Structural problems
37 that can affect the operation of a wind turbine could include delamination of the blade and failure
38 of tower and foundation systems. The foundation failure is often a slow process, developing
39 over a number of months or even years. However, recently, excessive vertical movement has
40 been reported in several onshore wind turbine concrete foundations with embedded ring as a
41 connection system [1]. These embedded rings have been recorded to be moving up to 20 mm or
42 more in some extreme cases and this could lead to catastrophic collapse of the turbines. Whilst
43 there is no published data on the exact number of failures due to commercial reasons, it is
44 thought that the problem is widespread given the popularity of the foundation system worldwide.

45 There are 4000 wind turbines of the type operational worldwide with further manufacturers also
46 using the foundation type.

47 SIM systems are widely used in various components, structures and sub systems of a wind
48 turbine to allow proactive maintenance and ensure reliability and availability of the machine [2].
49 For example, SIM systems have been applied to wind turbines to monitor blade delamination
50 using fibre optic sensors [3] and blade icing using thermal and acoustic sensors [4]. Wireless
51 monitoring technologies have also been suggested in order to limit the extra weight added to the
52 blade [5]. The turbine tower generally has an extremely low failure rate [6] and hence there has
53 been limited SIM applications. One study used strain gauge arrays to monitor the tower at a
54 number of locations from the bottom to the top of the tower [7]. The array layout meant changes
55 in tower modes due to wind direction could be monitored. In addition to new sensor
56 technologies, the application of wireless communication has made SIM more practical and
57 affordable. Research has been undertaken to assess the opportunities to apply wireless SIM to
58 many wind turbine parts including the rotor and tower [8].

59 There are a number of different foundations types used globally, and as foundations sizes
60 increase as turbines become larger, it becomes more important that foundations are designed and
61 monitored effectively, both during construction and throughout their operational lifetime [9].
62 However, currently there are no real time SIM systems in place for the operator to assist in its
63 monitoring of the problem, mapping or quantifying the movement patterns of the foundation and
64 subsequently alerting any potential failure.

65 In this paper, we present a wireless SIM system for onshore wind turbine concrete
66 foundations. First, a site investigation was conducted i) to identify the main damage
67 mechanisms responsible for the excessive vertical movement of the embedded ring, ii) to

68 determine the monitoring system requirements and iii) to develop movement alarm bands.
69 Then, a wireless sensor array system was designed and deployed in one wind turbine foundation
70 to monitor its vertical movement under normal turbine operating conditions. The reliability of
71 the monitoring system and the response of the individual sensors were assessed and compared to
72 SCADA data. The structural response of the concrete foundation was quantified under turbine
73 operational conditions and the effect of wind speed and direction on the vertical movement of the
74 foundation was analysed.

75 **2. Wind turbine test bed**

76 The onshore wind turbine concrete foundations with embedded ring shown in Fig. 1 are widely
77 used around the world. These types of foundations are the subject of this study with respect to
78 vertical movement. Several wind farms were visited to identify the main cause of this vertical
79 movement using Endoscopic filming through boreholes created in the foundations. The
80 Endoscopic filming showed significant voids filled with water under the flange of the embedded
81 ring. Significant erosion was also observed on the upper side of bottom flange due to the uplift
82 forces placed on the foundation by the rotor. These voids have caused excessive vertical
83 movement of the ring, leading to concrete cracking (Fig. 2) and failure of the water proofing
84 system.

85 Based on the site observations, the followings vertical movement bandings were used as
86 warning signals. Normal operation allows 1-2 mm of elastic stretching of the tower, 3-4 mm of
87 vertical movement is a sign that there is voids in the foundation and finally movement over 5
88 mm is deemed to be serious and further investigations are necessary. When the SIM records a
89 movement of 5 mm or greater, the foundation requires remediation. Accordingly, a sensor
90 sensitivity of 0.1 mm was adopted for the SIM system.

91 The wind turbine test bed used in this investigation was a modern 2.0 MW pitch regulated
92 variable speed machine and in operation for at least five years. The exact location and turbine
93 model are confidential due to a non-disclosure agreement with the operator. The foundation
94 consisted of an octagonal reinforced concrete slab with an embedded steel ring connection
95 system. Fig. 3 shows the geometry of the foundation. The foundation was designed to support a
96 67 m-hub tower equipped with a rotor of 80 m in diameter.

97 **3. Wireless SIM methodology**

98 Currently, monitoring of vertical movement involves visits by technicians to the site to take
99 manual readings of the foundation movement. This can be problematic during winter when the
100 site is often partially or fully inaccessible due to snow cover and/or high winds. Furthermore,
101 the greatest displacement occurs during higher wind speeds and this cannot be guaranteed during
102 each visit. Consequently, a SIM solution needed to allow more accurate and detailed real time
103 movement data. The SIM system presented in this paper was designed to provide a much greater
104 level of data to the engineering team than was previously available using site investigation
105 techniques alone.

106 In this project, linear variable differential transformer (LVDT) sensors were adopted to
107 measure the vertical movement of the embedded ring. LVDTs sensors are a very effective
108 method for measuring movement and have been used in a number of SIM applications in civil
109 engineering structures [10]. They are robust and immune to large magnetic field surrounding the
110 high voltage cables coiled in the foundation. LVDTs with a gauge length of 50 mm were
111 selected as being the optimum size and having a suitable accuracy for the displacement
112 measurements.

113 As shown in Fig. 4a, four LVDT sensors were installed under the top flange of the embedded
114 ring. Each LVDT was equipped with an off-the-shelf wireless communication node set to
115 measure displacement at a frequency of 1Hz. This rate was deemed to be sufficient for the
116 relatively slow movement of the turbine tower. The nodes were equipped with a 2.4 GHz
117 CC2420 wireless radio chip from Texas Instruments, which is IEEE 802.15.4 compliant. The
118 transmission power was set at 0 dBm while the receiver sensitivity of radio chip is -95 dBm.
119 The wireless gateway device consisted of an off-the-shelf low cost Raspberry Pi microcomputer,
120 a standard 4GB SD memory card and a small size battery pack, which acts as a UPS.

121 The sensors were positioned equidistant around the foundation (see Fig. 4a). The measurement
122 points are numbered on the figure as 1 NW (North West), 2 NE (North East), 3 SE (South West)
123 and 4 SW (South West). These points were selected because the prevailing wind conditions on
124 the site were south-westerly in nature. Using these measurement points, the sensor array would
125 capture the displacement on planes parallel and perpendicular to the prevailing wind. The LVDT
126 sensors were installed to measure the displacement between the static concrete foundation and
127 the embedded ring. It was essentially measuring the movement of the embedded ring at the
128 connection with the tower. Retort stands were used to keep the sensors with a heavy weight base
129 and the attachments were locked in position using thumbscrews, preventing any movement
130 during operation. The LVDTs were set half compressed, allowing vertical upwards and
131 downwards movements to be recorded. The LVDT installed in the foundation had a maximum
132 stroke of 50 mm; hence they were installed at a set position of 25 mm. Fig. 4-b shows the sensor
133 location along with the method of anchoring the sensor.

134 The monitoring of the foundation was carried out over a period of 2 months to evaluate the
135 performance of the SIM system under field conditions using a remote data acquisition system.

136 SCADA data was collected and correlated with the measured displacements. The data included
137 wind speed, wind direction and rotational speed of the rotor. Maximum and minimum wind
138 speed and standard deviations were obtained for each variable and used to evaluate the response
139 of the foundation under the turbine operating conditions. The recorded displacements were
140 compared with the maximum rotational speed since this was the key-influencing factor on the
141 displacement of the foundation

142 **4. Results and discussion**

143 *4.1. Effect of rotor and wind speed on the vertical displacement of the embedded ring*

144 Fig. 5a depicts the structural response of the embedded ring subjected to dynamic loading during
145 the turbine operating conditions over a period of 30 min. As can be seen, large drop offs in the
146 maximum rotor speed were observed. This was due to the drop in the wind speed. The standard
147 deviation of mean rotor speed exhibited peaks higher than 0.6, suggesting a period of turbulence.
148 The spikes in the ring displacement occurred in line with the standard deviation peak. This
149 means that during periods of turbulent wind, the rotor is subjected to sudden acceleration and
150 deceleration. This sudden change in the momentum resulted in the ring lifting and falling of the
151 embedded ring. This suggests that the embedded ring experiences vertical displacement during
152 sudden acceleration and deceleration of the rotor resulting from the change in the wind speed and
153 direction. Vertical displacement could also occur during shut down and start up events as this
154 produces sudden acceleration and deceleration of the rotor. Figure 5b shows a number of peak
155 displacements up to 5 mm. In this case, some of the peaks appeared to be related to the rotor
156 speed standard deviation e.g. turbulence, whilst others, such as at 19:12, appeared to be related to
157 the maximum rotor speed peaks.

158 As shown in Fig. 6, the embedded ring experienced significant vertical displacement at
159 high wind speeds. Serious displacement was deemed by the operator to be any movement over 5
160 mm in magnitude. Most of the vertical displacement was witnessed in the rising direction with
161 the tower settling back downwards after rotor speeds stabilised. A significant period of
162 displacement over approximately 5 min was observed between 18:00 and 18:05. The amber and
163 red warning lines at 3 mm and 5 mm respectively indicate the warning bands required by the
164 operator for analysis. At 18:01 there was a large drop off in the rotor speed, which triggered
165 large upward then large downward displacements of over 5 mm, breaching the red warning line.
166 Five small displacement peaks between 0.5 mm and 1.5 mm were also observed. Each of these
167 peaks correlated with the rotor speed standard deviation peaks as shown in Fig. 6.

168 High wind speeds also resulted in significant vertical displacement of the ring as indicated in
169 Fig. 7. This illustrates one of the many variable periods of displacement observed during the
170 monitoring period. As can be seen, rising and falling of the ring around 7 mm through 6
171 prescribed cycles were observed over a period of 15 min. The overall displacement pattern
172 correlated roughly with the maximum rotor speed peaks and troughs as well as with the mean
173 rotor speed standard deviation peaks. It is clear that there was a significant ring movement
174 tracking the significant fluctuation in the rotor speed, particularly between 19:18 and 19:25, with
175 a full cycle occurred approximately every minute. This cyclic (rise and fall) movement would be
176 evident to an observer on site. The displacement during this period travelled through all three
177 warning bands, resulting in red warning alerts, which would result in a warning alarm.

178 5.2. *Effect of wind direction on the vertical displacement of the embedded ring*

179 Figure 8a shows the effect of the wind direction on the vertical displacement of the embedded
180 ring. As shown, the southwesterly wind was turbulent causing rotor speed changes between 14.5

181 rpm and 16.5 rpm. As previously discussed, the displacement peaks correlated approximately
182 with periods of the high mean rotor speed standard deviation. The NW and SW sensors picked
183 up exactly the same movements. However, the sensor NW, orthogonal to the wind direction,
184 recorded larger displacements at every peak. This was the result of the wind direction and
185 ultimately the position of the rotor. It is likely that the side where the wind hit will be pushed up
186 a little but the greatest vertical movement was observed in the side where the rotor is rotating
187 upwards as a result of the uplift force experienced on the NW side of the foundation.

188 Figure 8b shows the displacement recorded by the NW, SW and SE sensors during a major
189 dip in the rotor speed. The NE sensor provided a corrupted signal. It appeared that the
190 displacement was variable around the circumference of the ring as a result of the wind direction
191 and the rotor uplift forces. The NW side of the ring exhibited higher displacement as compared
192 to SW and SE sides. The response of the sensor in the SE corner was slightly below zero much
193 of the time suggesting that the foundation has eroded allowing a negative displacement below the
194 level the sensors were set at.

195 **Conclusions**

196 The potential of using a low cost displacement sensor array to measure vertical movement of
197 onshore wind turbine foundations with embedded ring is presented in this paper. The system is
198 simple and relatively easy to install. The ability of the system to capture displacement,
199 regardless of wind direction demonstrates the potential for further development into a full SIM
200 system complete with user interface and alerting toolset. The site investigation identified
201 several damage mechanisms responsible for the excessive movement of the embedded steel ring.
202 Structural cracks were commonly observed in the concrete pedestals. Water ingress through
203 these cracks led to the formation of voids above and underneath the bottom flange of the

204 embedded ring. The cyclic movement of the embedded ring led the erosion of the concrete and
205 ultimately created these voids. The observed defects could have negative impact on the
206 structural integrity of onshore wind turbines and as a result, the development of renewable
207 energy could be hindered. Monitoring the progress of these defects is deemed necessary to
208 prevent catastrophic failures.

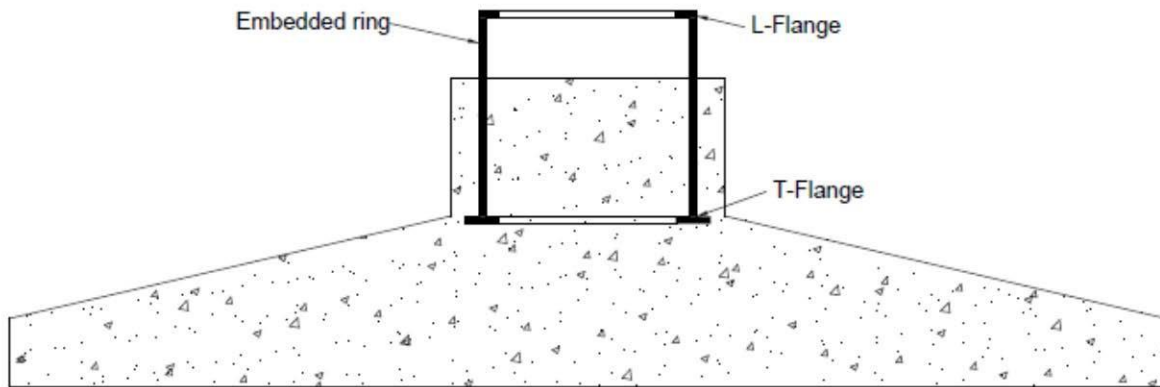
209 Based on the results from the field test, the wireless SIM system picked up a number of
210 varying movements including single and cyclic patterns. The Results also showed that the
211 embedded ring experienced vertical movement on a number of occasions (red warning 5mm or
212 greater movement). The excessive displacements were observed during periods of turbulent
213 wind speeds and during shut down and start up events. The wireless system presented herein
214 limited the number of cables in the turbine and allowed data download without need to access the
215 turbine. The system is flexible and could handle additional sensors, different sensors types and
216 also variable frequency of readings. The SIM system has the potential to greatly impact the
217 onshore wind energy industry by significantly reducing both the risk of catastrophic failure of the
218 foundations and the energy supply disruptions.

219 **References**

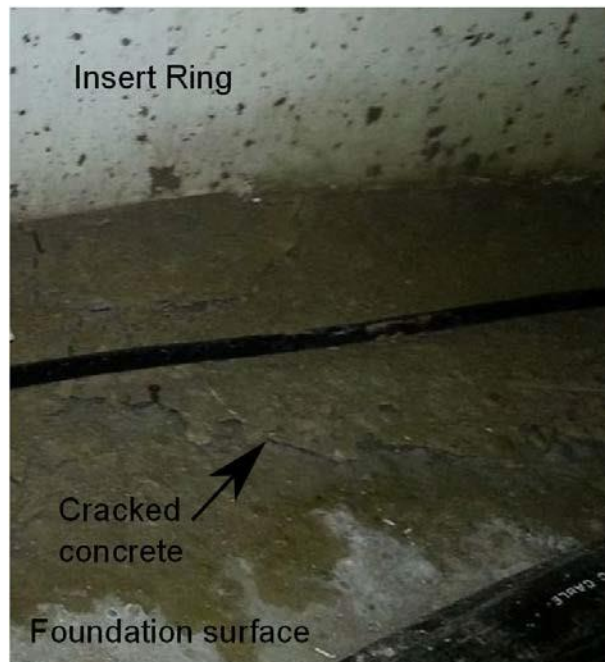
- 220 1. Currie M, Quail F, Saafi M. Development of a robust structural health monitoring system
221 for wind turbine foundations. in *ASME Turbo Expo 2012*. 2012. Copenhagen: ASME.
- 222 2. Schubel PJ, Crossley RJ, Boateng EKG, Hutchinson JR. Review of structural health and
223 cure monitoring techniques for large wind turbine blades. *Renewable Energy* 2013; 51:113-123.
224
225
- 226 3. Bang HJ, HK Shin, YC Ju. Structural health monitoring of a composite wind turbine
227 blade using fiber Bragg grating sensors, in *Sensors and Smart Structures Technologies for Civil,*
228 *Mechanical, and Aerospace Systems 2010*; Spie-Int Soc Optical Engineering: Bellingham.
229
230
231
232

233
234 4. Harper N. Detecting Ice on Wind-turbine Blades. Windpower Engineering 2011.
235
236 5. Taylor SG, Farinholt KM, Park G, Farrar CR, Todd MD. Application of a wireless sensor
237 node to health monitoring of operational wind turbine blades 2009; Conference: 28th
238 International Modal Analysis Conference ; February 1, 2010 ; Jacksonville, FL
239
240 6. Ribrant J, and Bertling LM. Survey of failures in wind power systems with focus on
241 Swedish wind power plants during 1997-2005. Ieee Transactions on Energy Conversion 2007;
242 22(1): 167-173.
243
244 7. Benedetti M, Fontanari V, Zonta D, Structural health monitoring of wind towers: remote
245 damage detection using strain sensors. Smart Materials & Structures 2011. 20(5).
246
247 8. Swartz RA, Lynch JP, Zerbst S, Sweetman B, Rolfes R. Structural monitoring of wind
248 turbines using wireless sensor networks. Smart Structures and Systems 2010; 6(3):183-196.
249
250 9 Wang P, Yan Y, Gui YT, Bouzid O, Ding Z. Investigation of Wireless Sensor Networks
251 for Structural Health Monitoring. Journal of Sensors, 2012; 2012.
252
253 10. Ciang CC, Lee JR, Bang HJ. Structural health monitoring for a wind turbine system: a
254 review of damage detection methods. Measurement Science & Technology 2008; 19(12).
255 11. Texas Instruments. Single-Chip 2.4 GHz IEEE 802.15.4 Compliant and ZigBee Ready
256 RF Transceiver (Rev. B) 2012 [cited 2013 Aug 4]; Available from:URL:
257 <http://www.ti.com/lit/ds/symlink/cc2420.pdf>.
258
259 12. Di Franco F, Tachtatzis C, Graham B, Bykowski M, Tracey DC, Timmons NF, Morrison
260 J. Current characterisation for ultra low power wireless body area networks. in Intelligent
261 Solutions in Embedded Systems (WISES) 2010; 8th Workshop on. 2010; 91-96.
262
263 13. RaspberryPi. Raspberry Pi FAQs 2013 [cited 2013 17th July]; Available from: URL:
264 <http://www.raspberrypi.org/faqs>.
265
266
267
268
269
270
271
272
273
274
275
276
277
278

279
280
281
282
283
284
285
286
287



288
289
290
291
292
293
294
295
296
297
298
299
300
301
302
303
304
305
306
307
308



309

310

311

312

313

314 Fig. 2 Cracked concrete foundation as a result of excessive displacement of the embedded ring.

315

316

317

318

319

320

321

322

323

324

325

326

327

328

329

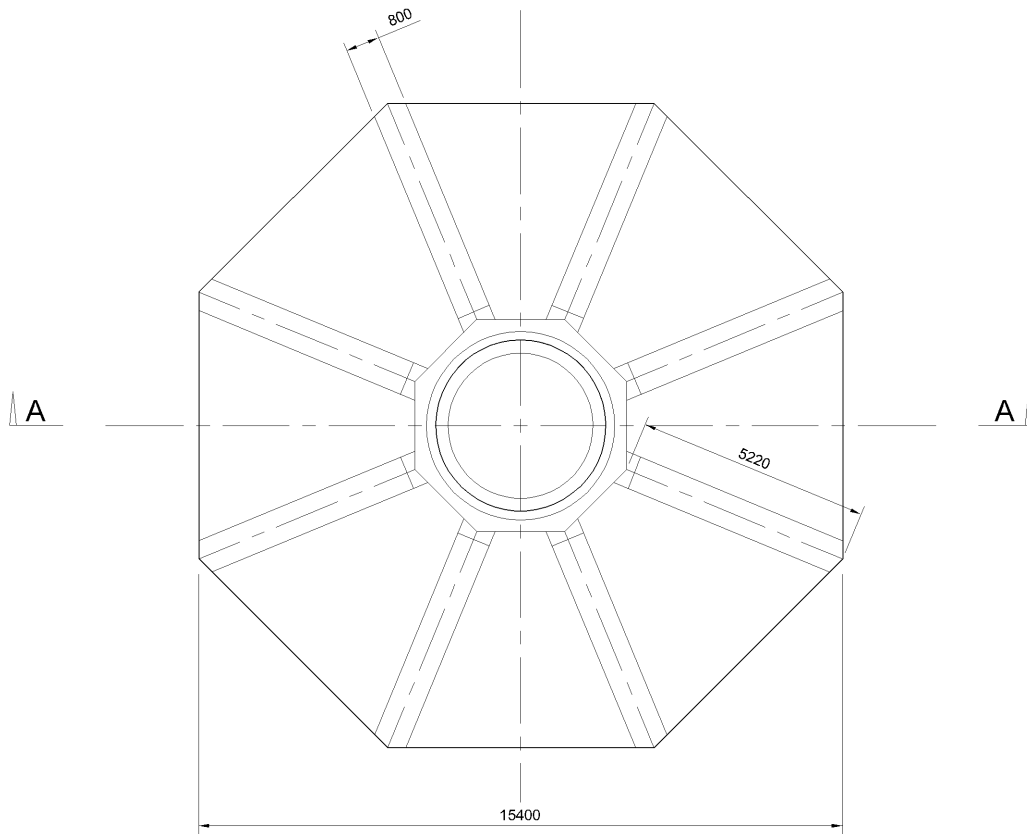
330

331

332

333

334



335 Plan

336

337

338

339

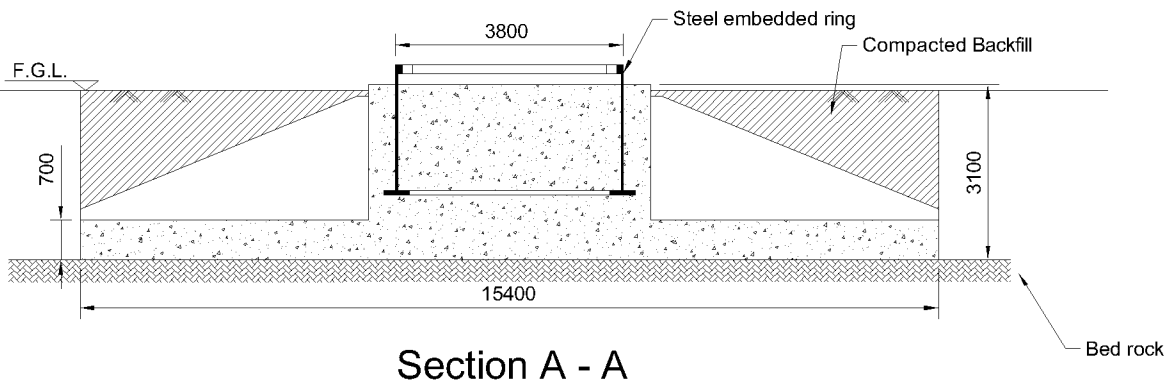
340

341

342

343

344



Section A - A

Fig. 3. Layout of the wind turbine concrete foundation (dimensions in mm)

345
346
347
348
349
350
351
352
353
354
355
356
357
358
359
360
361
362
363
364
365
366
367
368
369
370
371
372
373
374
375
376
377
378

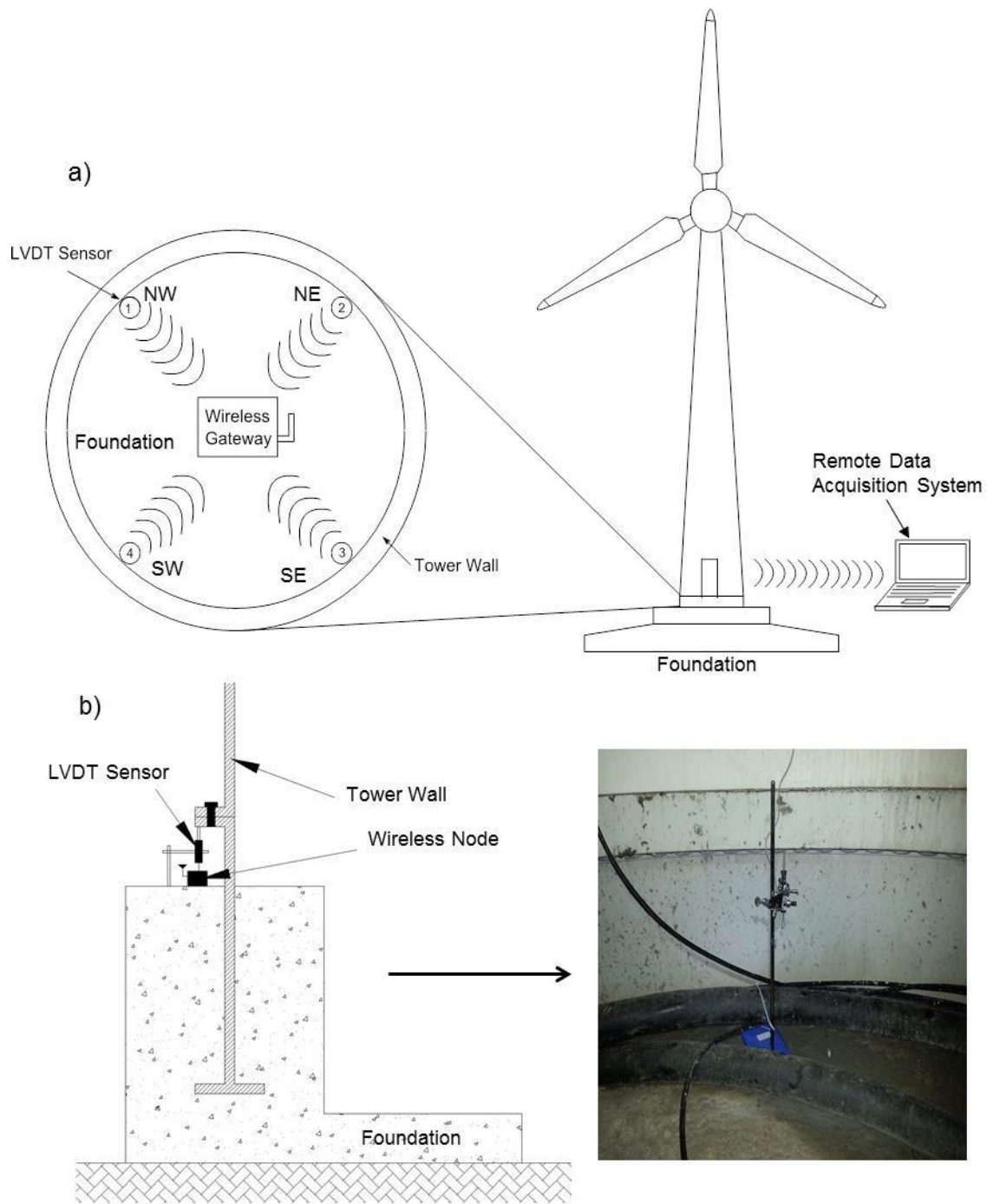
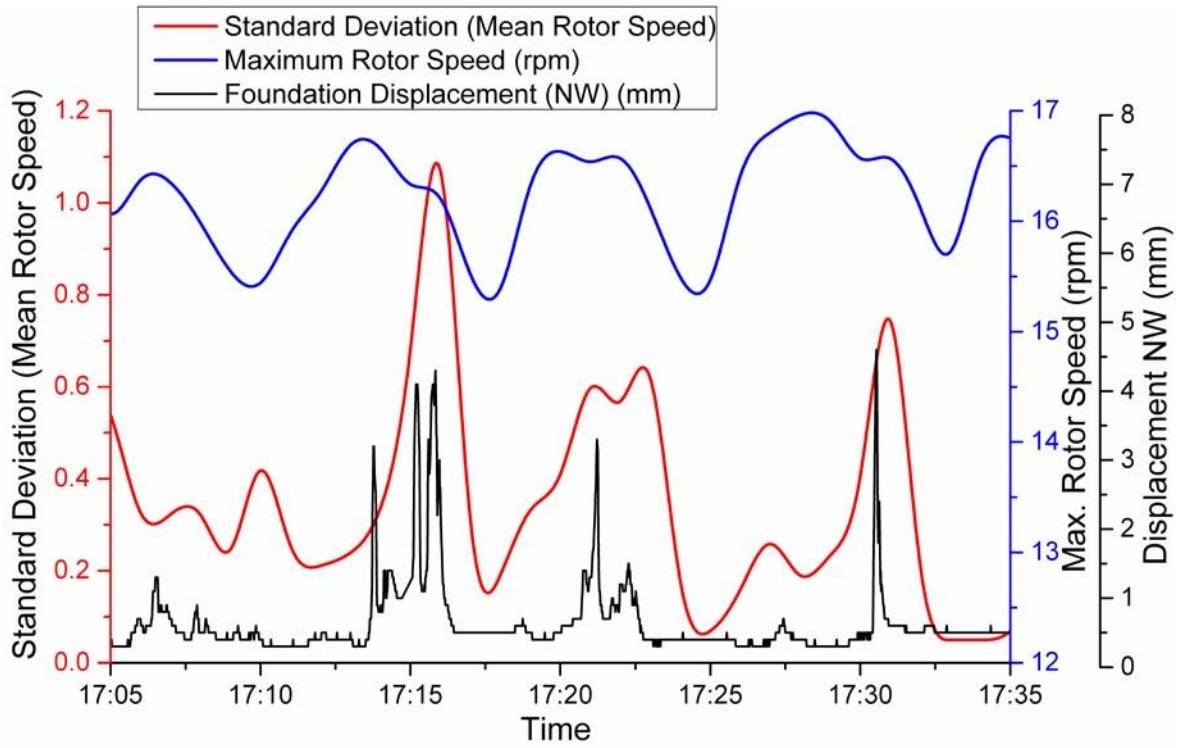


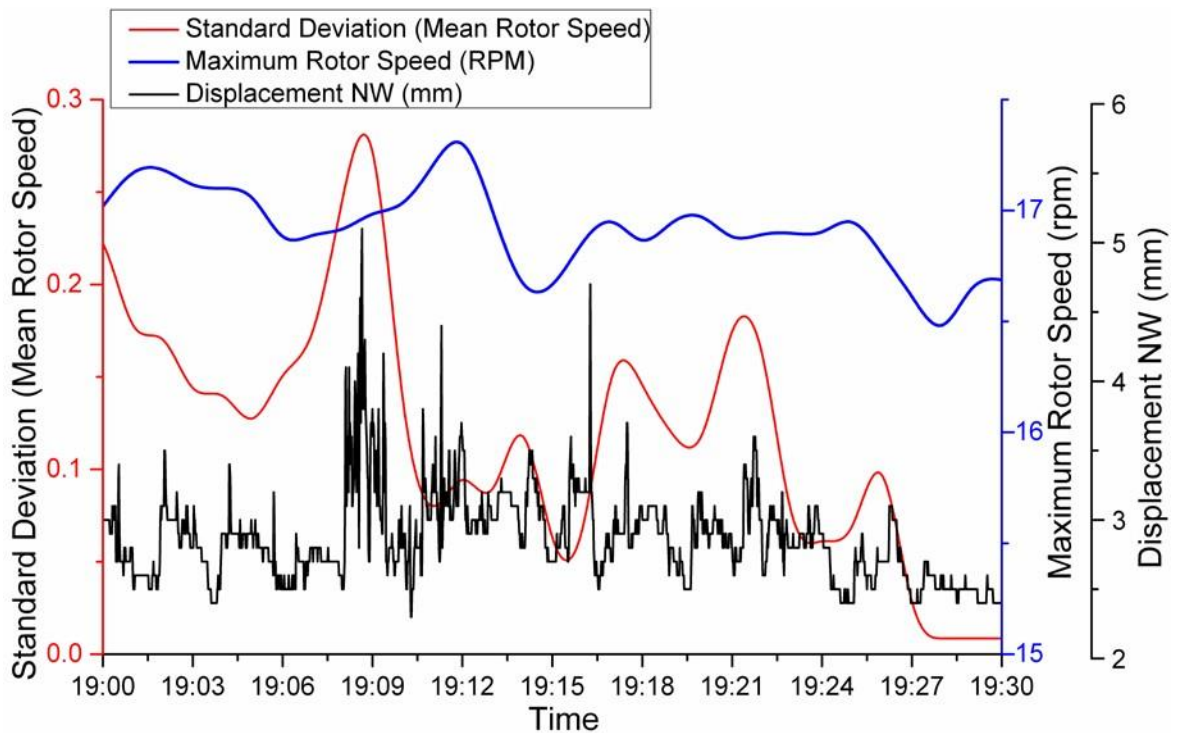
Fig. 4. a) SIM architecture and b) sensor installation.

379
380
381
382
383
384
385
386
387
388
389
390
391
392
393
394
395
396
397
398
399
400
401
402
403
404
405
406
407
408
409
410

a)



b)



411

412

413 Fig. 5. Effect of rotor speed on the vertical displacement of the embedded ring.

414

415

416

417

418

419

420

421

422

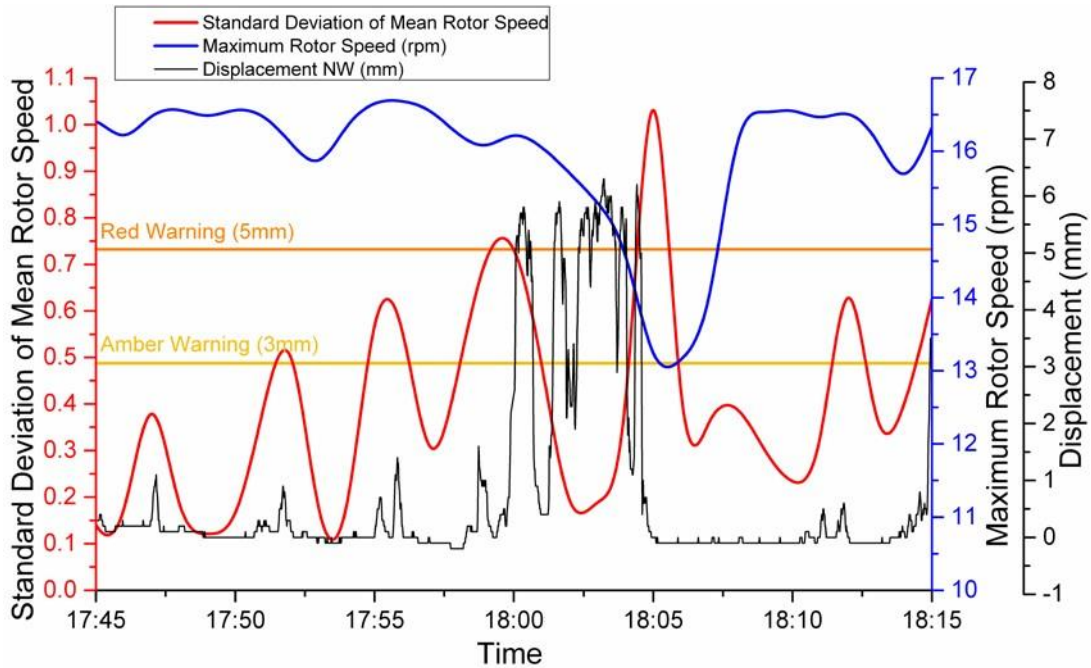
423

424

425

426

427



428 Fig. 6. Effect of high wind speed on the vertical displacement of the embedded ring.

429

430

431

432

433

434

435

436

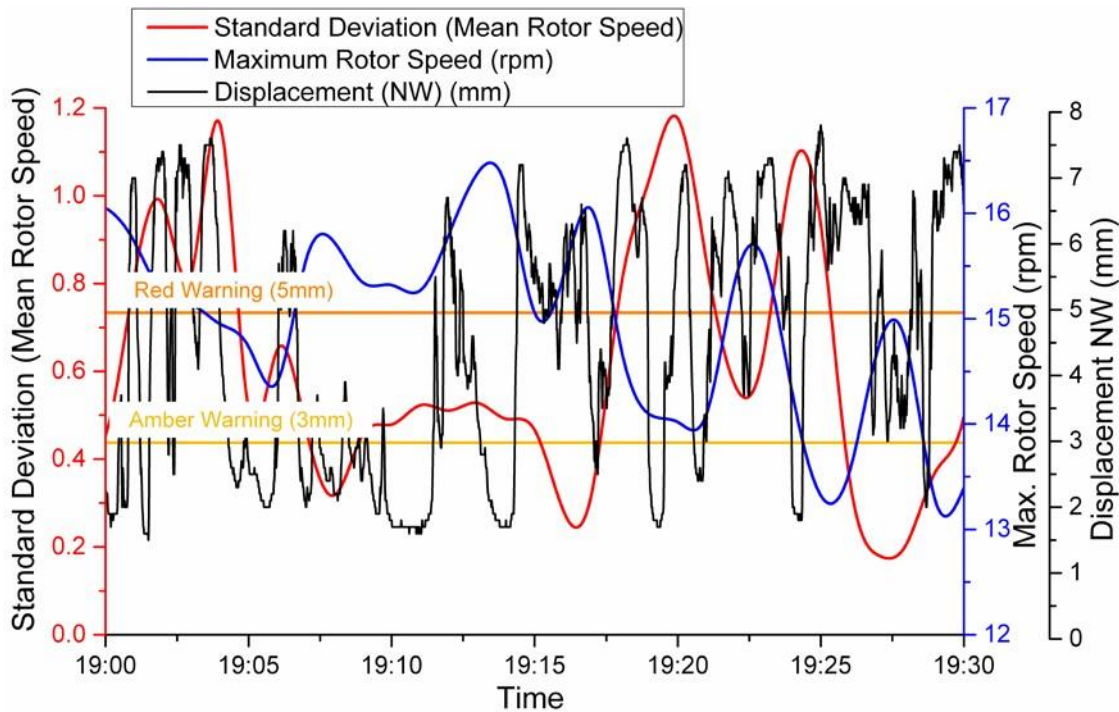
437

438

439

440

441



442

443

444 Fig. 7. Cyclic vertical displacement of the embedded ring as a result of high wind speed.

445

446

447

448 a)

449

450

451

452

453

454

455

456

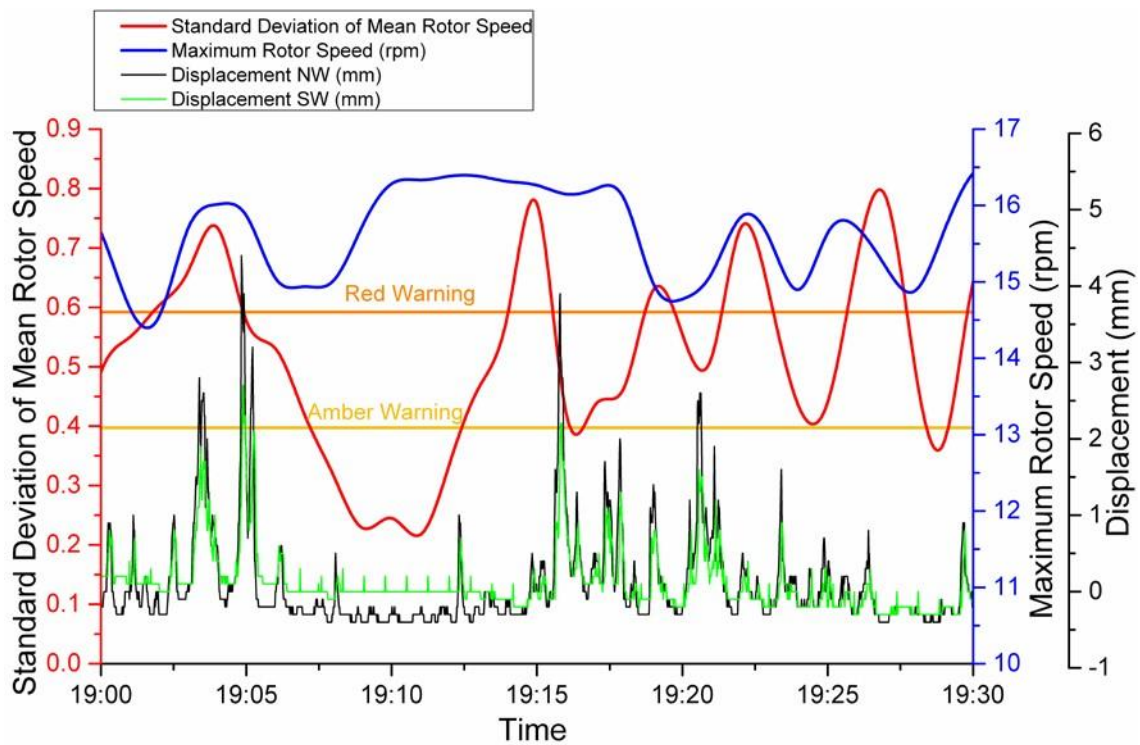
457

458

459

460

461



462

463 b)

464

465

466

467

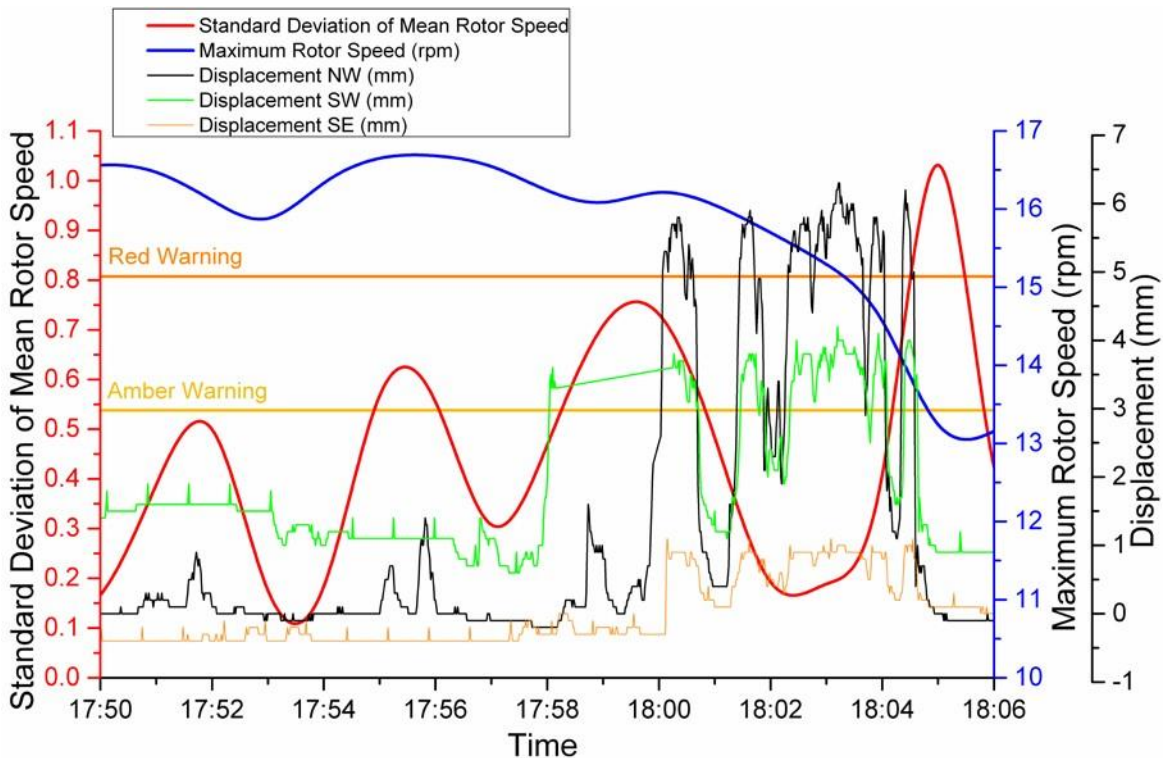
468

469

470

471

472



473

474

475 Fig. 8: Effect of wind direction on the vertical displacement of the embedded ring a) comparison
476 between NW and SW sensors, b) comparison between NW, SW and SE sensors during a major
477 change in the rotor speed.